Isomerization and unimolecular dissociation channels of the oxalic acid monomer

Charles W. Bock and Richard L. Redington

Citation: The Journal of Chemical Physics **85**, 5391 (1986); doi: 10.1063/1.451603
View online: http://dx.doi.org/10.1063/1.451603
View Table of Contents: http://scitation.aip.org/content/aip/journal/jcp/85/10?ver=pdfcov
Published by the AIP Publishing

Isomerization and unimolecular dissociation channels of the oxalic acid monomer

Charles W. Bock
Department of Chemistry and Physical Sciences, Philadelphia College of Textiles and Science, Philadelphia, Pennsylvania 19144

Richard L. Redington
Department of Chemistry and Biochemistry, Texas Tech University, Lubbock, Texas 79409

(Received 12 May 1986; accepted 24 June 1986)

The results of molecular orbital calculations performed for the oxalic acid monomer using the 6-31G, 6-31G*(5*d*), 6-31G**(5*d*), and MP2/6-31G*(5*d*) levels are reported. At the latter three levels of approximation the geometry with intramolecular hydrogen bonds is calculated to have the lowest energy, and the energies calculated for planar rotational conformers fall within about 2 kcal/mol of one another. The barrier hindering internal rotation of the carboxyl groups about the C–C bond for the nonhydrogen bonded conformer is calculated to be less than 1 kcal/mol, and secondary potential energy wells for *gauche*, rather than for the expected *cis*, carbonyl orientation are found about 300 cal/mol above the *trans* conformer at the 6-31G level. Vibrational frequencies calculated at the 6-31G level for the H-bonded conformer average about 9% higher than the observed values. On including electron correlation at the MP2 level the barrier calculated for the concerted, symmetrical, transfer of two protons between equivalent potential energy minima is 31.9 kcal/mol. This value is probably an upper bound. When electron correlation is ignored, calculations for the transfer of a single proton lead to a potential energy well that stabilizes an $(HO)_2CCO_2$ configuration with C_{2v} symmetry at an energy 26–28 kcal/mol above that of the H-bonded ground state conformer. When electron-correlation is included at the MP2 level there is a saddle point in the PES instead. This is the transition state for proton exchange by successive transfers, and a search for its position at the MP2 level was not made. However, energy values of 25.7 and 36.6 kcal/mol are calculated using MP2/6-31G*(5*d*) at optimized 6-31G critical point geometries, and these values are taken as temporary estimates for the MP2 level transition state energies for two-step proton exchange and for decarboxylation, respectively. It remains to be determined whether the stepwise proton exchange channel will be present for higher level calculations. The results of these MO calculations are consistent with the experimental observations of Lapidus, Barton, and Yankwich yielding first order kinetics, a low activation energy (31.5 kcal/mol), and complex kinetic isotope effects for the thermal decarboxylation of the oxalic acid monomer. Because of its importance in this reaction, calculations of the 1,2 H atom shift of dihydroxycarbene are also reported.

I. INTRODUCTION

Unimolecular reaction channels that are conceivable for the oxalic acid monomer include rotational isomerizations, intramolecular proton exchanges, and several dissociation reactions, but not much is known experimentally or theoretically about this interesting molecule. Electron diffraction analysis,[1,2] and vibrational[2–8] and UV[9] spectroscopic studies have been most often interpreted in terms of structure I, the intramolecular hydrogen bonded conformer with C_{2h} symmetry. The character of presumably higher energy conformers, e.g., structure II, and the nature of conformational transitions are not known.

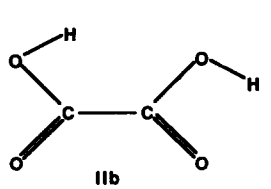

IIb

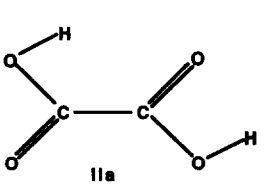

IIa

Some of these properties are addressed in the present article using molecular orbital theory with relatively large basis sets. In addition, unimolecular dissociation of the molecule is addressed since oxalic acid is unstable and the kinetics of thermal dissociation of oxalic acid isotopomers in the vapor phase to form formic acid and CO_2 have been studied.[10–13] Dissociation by UV radiation, mercury ($^3P_1$)-photosensitized decomposition, and dissociation through CO_2 laser multiphoton absorption have also been recently reported.[14] To our knowledge only a single *ab inito* calculation has been previously reported in the literature for oxalic acid monomer.[15] This provides the optimized geometry of the hydrogen bonded conformer I at the 4-31G basis set level. In this article we present the results of molecular orbital calculations carried out using the more complete 6-31G, 6-31G*(5*d*), and 6-31G**(5*d*) basis sets as well as introducing electron correlation corrections at the MP2 level. These calculations were performed to provide reasonable theoreti-

TABLE I. Optimized geometries[a] of $C_2O_4H_2$ configurations calculated using 6-31G basis.

Bondlength or angle	I[a]	II	II_a[b]	II_b	III	IV	V_a	V_b	V_c	DHC[c] CO_2	DHC[†]	VI
O_3H_1	0.957	0.955	0.954	0.954	1.289	1.339	0.961	0.969	0.956	0.949	0.950	0.960
			0.954	0.955			1.160				1.234	0.979
C_5O_3	1.325	1.335	1.315	1.338	1.252	1.268	1.284	1.272	1.297	1.329	1.320	1.279
			1.305	1.352			1.274				1.283	1.281
$C_6{=}O_8$	1.204	1.203	1.176	1.196	1.252	1.268	1.215	1.234	1.191			1.214
			1.189	1.197			1.246			1.161		1.249
C_5C_6	1.519	1.510	1.535	1.518	1.518	1.475	1.555	1.567	2.031			1.606
$\angle C_5O_3H_1$	116.1	114.5	110.4	116.4	94.2	70.8	115.1	112.2	113.7	113.4	115.5	118.9
			109.1	115.6			97.4				59.0	110.0
$\angle C_6C_5{-}O_3$	115.0	111.5	112.1	115.5	109.6	125.4	124.2	120.3	123.6			125.6
			113.6	110.7			104.6					115.8
$\angle C_5C_6{=}O_8$	120.4	124.2	120.8	121.3	109.6	125.4	118.1	110.5	103.1			115.9
			123.1	124.8			110.7					105.6
$\angle O_3C_5O_7$	124.6	124.4	124.8	123.2	140.8	109.2	125.1	119.5	112.8	105.8	118.1	118.6
			125.6	124.5			138.6	139.0	153.8	180.0		138.5

[a] Units: distances in angstroms, angles in degrees, atom numbers in Fig. 1; diagrams illustrating configurations are given in the text.
[b] 6-31G*(5*d*) basis; two parameter values, with atom numbering given for the first, are listed for asymmetric configurations.
[c] DHC = dihydroxycarbene; DHC[†] = transition state for 1, 2 H shift.

cal estimates for the geometries and energies of the more general $C_2O_4H_2$ conformations, and the energetics of proton transfers and dissociation channels. The results bear strongly on interpretations of the extant experimental observations on oxalic acid monomer and they provide a degree of stimulation for the course of future experiments.

II. COMPUTATION METHODS

The Gaussian 82 code with its standard optimization routines for a VAX 11/780 computer[16] were used for all calculations. The runs utilized the built-in 6-31G, 6-31G*(5*d*), and 6-31G**(5*d*) basis sets as these have provided good geometries and reasonable vibrational frequencies, relative energies, and other properties for the formic acid monomer,[17] which is relevant to this research, and similar molecules that have been studied at these levels.[18] Single point MP2/6-31G*(5*d*)||HF/6-31G (energy||geometry) calculations were also carried out for some conformers and at critical points along the decarboxylation reaction profile to assess the effect of electron correlation on the relative energies.[19]

III. RESULTS

A. Rotational conformers

Complete geometry optimizations were performed for conformers I and II and, inspired by the 1 cm^{-1} value for the C–C torsional vibrational frequency that is calculated for conformer II (next section), for internal rotation of planar carboxyl groups of conformer II about the C–C bond. The geometrical parameters obtained for conformers I and II in these calculations are listed in Table I (6-31G) and Table II

TABLE II. Optimized geometries[a] of $C_2O_4H_2$ configurations calculated using 6-31G**(5*d*) basis.

Bond length or angle	I(obs.[b])	I[a]	II	III	IV	V_a[c]	V_b	DHC[d] CO_2
O_3H_1	1.056(0.014)	0.951	0.948	1.252	1.283	0.956	0.965	0.943
						1.11		
C_5O_3	1.339(0.002)	1.303	1.314	1.233	1.240	1.268	1.256	1.307
						1.229		
$C_6{=}O_8$	1.208(0.001)	1.184	1.181	1.233	1.240	1.197	1.213	1.143
						1.245		
C_5C_6	1.548(0.004)	1.535	1.532	1.504	1.508	1.555	1.571	
$\angle C_5O_3H_1$	104.4(2.3)	110.0	108.7	90.7	71.1	108.4	105.7	108.2
						93.8		
$\angle C_6C_5{-}O_3$	111.9	114.0	111.2	109.9	124.2	123.6	119.9	
						111.3		
$\angle C_5C_6{=}O_8$	123.1(0.9)	120.5	123.4	109.9	124.2	117.4	110.2	
						104.7		
$\angle O_3C_5O_7$	125.0(0.2)	125.5	125.4	140.2	111.6	125.1	120.2	105.5
						137.9	139.6	180.0

[a] Units: distances in angstroms, angles in degrees, atom numbers in Fig. 1; diagrams illustrating configurations given in the text.
[b] Electron diffraction results of Ref. (2).
[c] An almost optimized geometry (internal coordinate forces no worse than twice the normal cutoff threshold value); two parameter values, with atom numbering given for the first, are listed for asymmetric configurations.
[d] DHC = dihydroxycarbene.

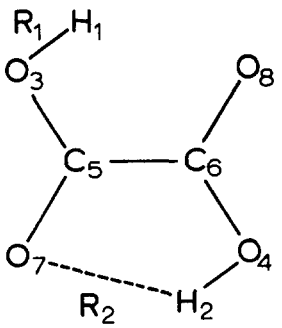

FIG. 1. Atom numbering used for coordinates in Tables I and II and in Figs. 3 and 4.

[6-31G**(5*d*)] using the atom numbering shown in Fig. 1. Experimental values reported by Nahlovska *et al.*[2] in their 1970 electron diffraction study are also included in Table II. These authors could not reliably distinguish between the calculated fits provided by conformers I and II to their electron diffraction data, but chose conformer I because the low value observed for the OH stretching mode in the infrared spectrum suggests intramolecular H-bonding. Comparison of the observed and calculated geometries listed in Table II suggest that the strength of the H-bonding remains underestimated at the 6-31G**(5*d*) level, where it is nevertheless strong enough to lower the energy calculated for conformer I below that of conformer II. The calculated energies of conformers I and II differ very little for the basis sets investigated, as seen in Tables III and IV and in Fig. 2. At the 6-31G level conformer II is calculated to be 0.5 kcal/mol lower in energy than conformer I; however, at the 6-31G**(5*d*) level conformer II is 2.0 kcal/mole higher in energy than conformer I. The value is nearly the same, 1.9 kcal/mol, for the MP2/6-31G*(5*d*)||HF/6-31G calculation as seen in Table IV. These MO results suggest a Boltzmann factor of about 0.08 at 130 °C. This value is compatible with a preponderance of conformer I in samples used for the experimental studies, and also with the observation of "extra" absorption bands in infrared matrix isolation studies[7,8] that can be attributed to secondary conformers of oxalic acid monomer trapped from the warm vapor into the cold matrix solid.

The above calculations demonstrate the importance of including polarization functions in basis sets used for oxalic acid monomer, particularly when intramolecular hydrogen bonding is of concern, and suggest that the stabilization of conformer I provided by two intramolecular hydrogen bonds is strongly compensated by the increase in energy associated with the formation of two *trans* HO/C=O carboxyl configurations. For the case of formic acid monomer the potential energy minimum of the *trans* HO/C=O conformer is reported to occur 4.09 kcal/mol above the minimum for the *cis* configuration on the basis of relative intensities of microwave transitions.[20] *Ab initio* calculations provide corroborating *trans-cis* energy differences that are, however, considerably larger than this (6.8 kcal/mol for 6-31G basis[17]). The barriers hindering internal rotation of the OH groups of oxalic acid monomer were not calculated, however, energies of the singly hydrogen bonded structures

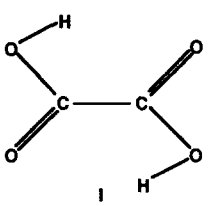

I

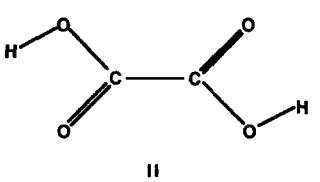

II

were calculated at the 6-31G*(5*d*) and 6-31G levels, respec-

TABLE III. Energies of $C_2O_4H_2$ conformations in hartrees.

Structure	G||G[a]	G*||G	G**||G**	MP2||G
I	−376.170 01	−376.362 39	−376.382 03	−377.304 35
		[−376.367 73][b]		
II	−376.170 76	−376.359 05	−376.378 92	−377.301 36
II_a		[−376.365 25][b]		
II_b	−376.168 45			
III	−376.070.03	−376.278 50	−376.301 90	−377.253 58
IV	−375.971 01	−376.184 68	−376.211 55	−377.183 44
V_a	−376.111 64	−376.311 78	−376.333 57	−377.267 08
V_b	−376.125 21	−376.320 69	−376.341 11	−377.263 43
V_c	−376.111 91	−376.307 61		−377.245 99
VI	−376.111 51			
DHC[c] + CO_2	−376.116 58	−376.319 02		−377.247 15
DHC[†] + CO_2	−376.014 26			
cis-FA + CO_2	−376.169 67			
trans-FA + CO_2	−376.180 44		−376.403 18	
DHC	−188.601 62	−188.686 98		−189.148 06
DHC[†]	−188.499 30	−188.596 03		−189.093 32
cis-FA	−188.654 72			
trans-FA	−188.665 49		−188.769 66	
CO_2	−187.514 95	−187.632 04	−187.633 52	−188.099 08

[a] G = HF/6-31G; G* = HF/6-31G*(5*d*); MP2 = MP2/6-31G*(5*d*); energy||geometry.
[b] G*||G* value.
[c] DHC = dihydroxycarbene "*W*" conformer (Fig. 5); DHC[†] = 3-center transition state (Fig. 6); FA = formic acid.

TABLE IV. Energy differences of $C_2O_4H_2$ conformations in kcal/mol.

Structure	$E-E_I$				$E-E_{V_b}$			
	G‖G[a]	G*‖G	G**‖G**	MP2‖G	G‖G	G*‖G	G**‖G**	MP2‖G
I	0	0	0	0				
II	− 0.47	2.1	2.0	1.9				
II_a		1.6						
II_b	1.0							
III	62.8	52.6	50.3	31.9				
IV	124.9	109.4	107.0	74.0				
V_a	36.6	31.8	30.4	23.4	8.5	5.6	4.7	− 2.3
V_b	28.1	26.2	25.7	25.7	0	0	0	0
V_c	36.5	34.4		36.6	8.4	8.2		10.9
VI	36.7				8.6			
DHC[b] + CO_2	33.5	27.2	27.7	35.9	5.4	1.0	1.5	10.2
DHC[†] + CO_2	97.8	84.3		70.3	69.7			
cis-FA + CO_2	0.2							
trans-FA + CO_2	− 6.5		− 13.3					
DHC	0[c]	0		0				
DHC[†]	64.2	57.1		34.4				
cis-FA	− 33.3							
trans-FA	− 40.1							

[a] G = 6-31G, G* = 6-31G*(5*d*), G** = 6-31G**(5*d*), MP2 = MP2/6-31G*(5*d*); energy ‖geometry.
[b] DHC = dihydroxycarbene *W* conformer (Fig. 5); DHC[†] = 3-center transition state (Fig. 6); FA = formic acid.
[c] The following energies are relative to dihydroxycarbene.

tively. Their energies are less than 2 kcal/mol higher than that of conformer I when the latter is investigated using the same basis set. These energies are included in Tables III and IV and the geometries are listed in Table I.

Calculations at the 6-31G level for the barrier hindering internal rotation of the carboxyl groups about the C–C bond of conformer II lead to the results that: (a) the internal rotation barrier is less than 1 kcal/mol; (b) a secondary potential energy minimum arises for a 30°–40° out-of-plane *gauche* orientation rather than for the expected planar *cis* carbonyl orientation. At the 6-31G**(5*d*) level the planar *cis* form is also found to be less stable than a *gauche* structure with a 30° twist angle. The *trans–gauche* energy difference at this angle is nearly double that found using the 6-31G basis set. The potential energy function for this internal rotation was determined with full geometry optimization for planar carboxyl groups and 30° sampling intervals for the dihedral angle. The results are given in Fig. 2 and Table V. A reasonable least-squares fit of the usual cosine series to the calculated points requires four parameters and yields

$$V = 97.7(1 - \cos\theta) + 342.2(1 - \cos 2\theta) + 109.2(1 - \cos 3\theta) - 131.1(1 - \cos 4\theta)$$

where θ is the O=C–C–O dihedral angle, the units are cal/mol, the primary maximum (0.90 kcal/mol) occurs at 86°, the secondary minimum occurs at 143° (*gauche* structure, 0.25 kcal/mol, 37° out-of-plane), and the seven points are fitted with an average deviation of 6%.

Although experimental evidence concerning oxalic acid is lacking, the shape of the potential energy function calculated for conformer II very strongly resembles that reported

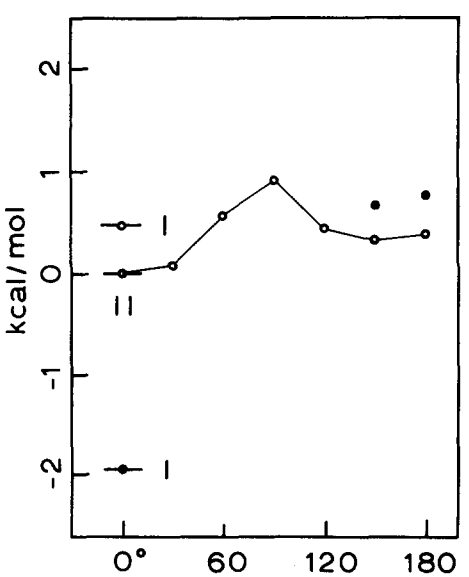

FIG. 2. Relative energies of $C_2O_4H_2$ conformers I and II and internal rotation about the C–C bond for conformer II. Open circles are for the 6-31G basis set; filled circles are for the 6-31G**(5*d*) basis set.

TABLE V. Internal rotation about C–C bond by conformer II.[a]

	Angle	6-31G		6-31G**(5*d*)	
		a.u.	kcal	a.u.	kcal
I		− 376.170 01	+ 0.48	− 376.382 03	− 1.96
II	0 (*trans*)	− 376.170 76	0	− 376.378 92	0
	30	− 376.170 62	0.09		
	60	− 376.169 84	0.58		
	90	− 376.169 31	0.91		
	120	− 376.170 07	0.43		
	150	− 376.170 27	0.31	− 376.377 85	0.67
	180 (*cis*)	− 376.170 14	0.39	− 376.377 72	0.75

[a] O=C–C–O dihedral angle.

for oxalyl fluoride by Godunov *et al.*[21] on the basis of their analysis of the vibronic structure observed in UV spectra of the vapor. Oxalyl fluoride and oxalic acid are isoelectronic, and the large negative value for V_4, the $(1-\cos 4\theta)$ coefficient, particularly stands out in both of the internal rotation potential energy functions under discussion. The primary maximum for the oxalyl fluoride potential function is about 2.8 kcal/mol above the *trans* minimum. The *gauche* minimum is 0.70 kcal/mol above the *trans* minimum, occurs for a F–C–C=O dihedral angle of about 25°, and lies only a few cal/mol below the secondary maximum at 180° (cf. Fig. 1 for oxalic acid conformer II). *Ab initio* calculations on oxalyl fluoride at the 6–31G level[22] yield a barrier height (at 90°) almost twice the experimental value just cited and the secondary potential minimum, calculated to lie about 500 cal/mol above the *trans* potential energy minimum, has *cis* rather than *gauche* geometry.

Glyoxal lacks the sizable V_3 and V_4 internal rotation potential function terms that arise when its H atoms are replaced with F or OH. Glyoxal has a planar *cis* secondary conformer lying in a well-defined potential well about 5.5 kcal/mol[23] above the low energy *trans* form.

B. Harmonic vibrational frequencies

Harmonic estimates for the vibrational frequencies of oxalic acid monomer were calculated for conformers I and II using the FREQ = NUMER option at the 6-31G level. The results are listed in Table VI, along with the observed values. The extremely low frequency calculated for the C–C torsional mode of conformer II particularly stands out, along with a number of relatively large frequency shifts between I and II that are evidently associated with opening the intramolecular hydrogen bonds of conformer I. The vibrational spectrum of oxalic acid monomer is discussed in detail in a separate article that includes infrared matrix isolation observations on H, C, and O isotopomers.[8] In that work the vibrational force field of conformer I is estimated using calculations that combine the observed isotopomer frequencies with force constant constraints imposed by the present 6-31G level MO calculations.

At present, the following points are made. It is noted that the vibrational frequencies calculated using the 6-31G basis set average about 9% higher than the observed values, as seen in Table VI. This general information is used to suggest values for three Raman active modes that have not been directly observed. Very tentative values are proposed for ν_6 and ν_{11} on the basis of their occurrence in (reassigned) combination modes observed in the infrared spectra and their compatibility with the values presently calculated using MO theory. More firmly, with respect to the B_g Raman mode ν_{12}, important infrared transitions are observed at 1329, 1273, and 1138 cm^{-1}.[7,8] Only two of these bands can be attributed to fundamental modes. Infrared spectra of carbon and oxygen isotopomers support the assignment of 1329 and 1138 cm^{-1} as the fundamentals and the third band as the combination mode between the two OH torsional fundamentals $\nu_8 + \nu_{12}$.[8] The resulting value of 609 cm^{-1} insinuated for ν_{12} is compatible with the value calculated using MO theory and with the presence of a Raman band at 590 cm^{-1} for oxalic acid dissolved in methanol[3] and 575 cm^{-1} for aqueous solvent.[5]

C. Symmetrical intramolecular proton exchange

Optimized geometries and energies for structures III and IV of D_{2h} symmetry are listed in Tables I–IV and compared with energies for other structures in Fig. 3.

TABLE VI. Fundamental vibrational frequencies of oxalic acid monomer conformers I and II, 6-31 G basis set.

No.	Sym.	Obs.[a]	I (calc./obs)	I (calc.)	II (calc.)	Approx. descript.[b]
1	A_g	...	...	3954.8	3996.0	νOH
2		1800	1.10	1978.9	1974.1	νC=O
3		1423	1.06	1506.4	1561.8	νCO/δCOH
4		1195	1.09	1307.3	1278.8	δCOH/νCO
5		815	1.09	886.0	859.6	νCC/δOCO/δCOH
6		(538)[c]	(1.13)	606.4	580.3	COOH rock
7		405	1.11	450.8	465.9	COOH def.
8	A_u	664	0.97	646.0	679.2	τCOH
9		461	1.08	498.7	467.0	CO_2wag
10		89	1.39	124.0	1.0	τCC
11	B_g	(810)[c]	(1.05)	847.8	892.1	COOH wag
12		(609)[c]	(1.04)	630.9	622.5	τCOH
13	B_u	3472	1.14	3955.3	3995.3	νOH
14		1817	1.09	1971.9	1929.1	νC=O
15		1329	1.02	1352.7	1449.7	νCO/δCOH
16		1138	1.13	1291.1	1215.4	δCOH/νCO
17		651	1.11	722.1	635.4	δOCO
18		264	1.11	291.8	299.3	COOH rock

[a] Units are cm^{-1}. IR transitions from Ref. 7; Raman transitions from Ref. 6; ν_{10} from Ref. 9.
[b] ν = stretch, δ = angle bend; τ = torsion.
[c] From IR combination mode.

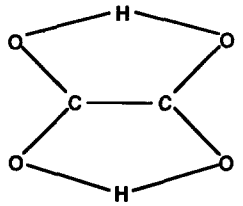

III

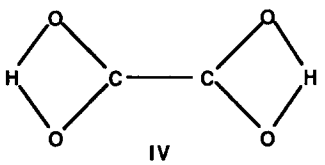

IV

These calculations yield maxima for the energy barriers hindering symmetrical, concerted, transfer of the protons in conformers I and II of 50.3 and 107.0 kcal/mol, respectively, at the 6-31G**(5*d*) level. The values are lowered to 31.9 and 74.0 kcal/ml, respectively, when electron correlation is included at the MP2/6-31G*(5*d*) level with the 6-31G level geometries. These changes are much larger than those obtained for analogous calculations on other conformers.

Using polarization functions and including electron correlation produces a large decrease in the calculated energy difference between conformer I and III (or IV), which have configurations that are highly distorted from normal molecular geometries (cf. Tables I–IV). The calculated barrier between conformers III and I (which is likely to be an upper bound because of the symmetry and the relative correlation energy contributions to the energies of III and I) suggests the possibility for future observation of biprotonic tunneling phenomena in oxalic acid monomer. No experimental evidence concerning intramolecular proton transfer for oxalic acid has yet been reported.

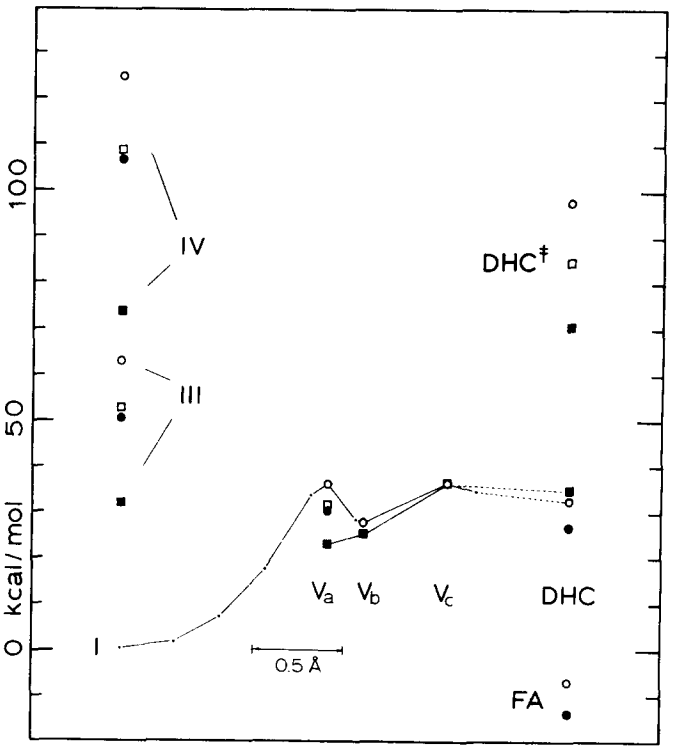

FIG. 3. Relative energies of $C_2O_4H_2$ and $(HO)_2C$: conformers showing values as a function of the original $O_7\cdots H_2$ distance R_2 of the transferred proton for transformation $I \rightarrow V_b$, and of the C–C distance for transformation $V_b \rightarrow V_c$. Also indicated are the energy of CO_2 plus dihydroxycarbene ("*W*" isomer) = DHC, *trans* formic acid FA, and the transition state DHC‡ for the reaction DHC→*cis*-FA. Open circles = G/G; filled circles = G**/G**; open squares = G*/G; filled squares = MP2/G (cf. Table IV).

D. Single proton transfer and symmetrical $(HO)_2CCO_2$ configurations

The possibility that single proton transfers can occur was considered, first at the SCF level and then using MP2 to assess the effect of electron correlation. The SCF calculations produced the following critical point configurations, where structures V_b and V_c have C_{2v} symmetry.

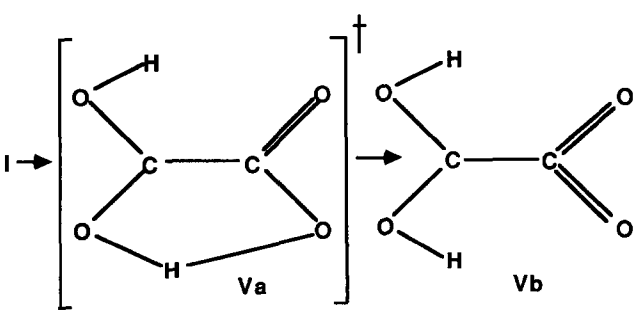

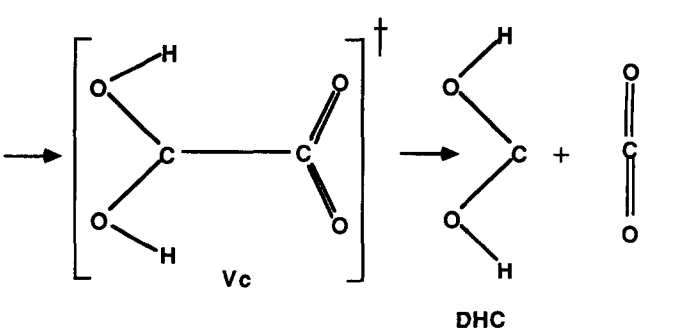

Starting with conformer I, the energy was minimized with complete optimization of planar geometries using the R_2 bond distance shown in Fig. 1 as a parameter. The resulting potential energy valley led to the determination of transition state V_a and to a potential energy minimum for conformer V_b. At the 6-31G**(5*d*) level the transition state energy is only 30.4 kcal/mol above that of conformer I and 4.7 kcal/mole higher than that of conformer V_b, $(HO)_2CCO_2$. The results of these calculations appear in Tables I–IV. The reaction profile leading from I to V_b is indicated in Fig. 3, where

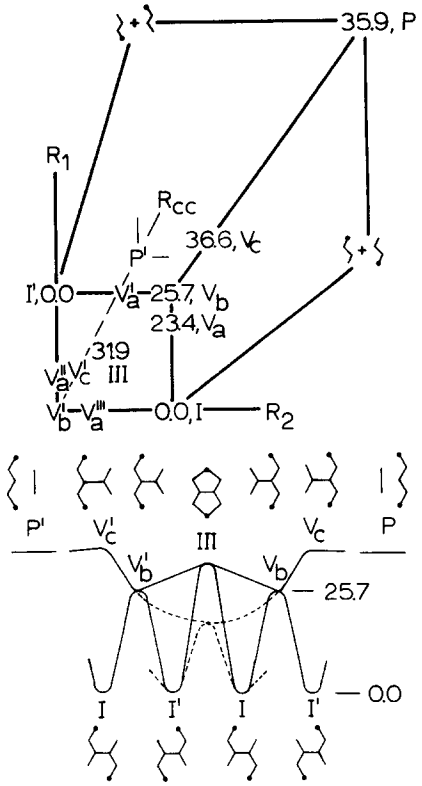

FIG. 4. Representation of MP2 level energy points in three-dimensional coordinate space for $R_1 = O_3H_1$, $R_2 = O_7H_2$, and R_{CC} (cf. Fig. 1). Relative energies are connected by schematic reaction profiles in the lower portion of the figure. The dotted curves represent the hypothetical case arising when the energy of III is lower than that of any species with C_{2v} symmetry. In this case, III becomes a saddle point, and V_b is no longer a critical point.

points along the minimum energy path are plotted as a function of R_2, the parametric $O_7\cdots H_2$ distance.

The segment of the reaction profile leading from $(HO)_2CCO_2$, V_b, to dissociation products was also investigated at these basis set levels. Starting with conformer V_b, the energy was minimized for complete optimization of planar geometries using the C–C bond distance as a parameter. It was found that $(HO)_2CCO_2$ dissociates through a low energy transition state V_c to form dihydroxycarbene (DHC) and CO_2. At the 6-31G**(5*d*) level the activation energy is 8.4 kcal/mol (only 36.5 kcal above the energy of conformer I). The products dihydroxycarbene and CO_2 are calculated to be 5.4 kcal/mol above the energy of conformer V_b. These results appear in Tables I–IV and Fig. 3.

When electron correlation is included by performing MP2/6-31G*(5*d*)||HF/6-31G calculations for configurations V_a, V_b, and V_c, the potential energy well stabilizing V_b no longer exists as shown in Fig. 3 and Table IV. It is not possible to map the potential energy surface for oxalic acid monomer in great detail at present, but its important features are highlighted using available MP2 energies and SCF geometry optimizations in the three dimensional representation based on OH and CC bond distances shown in Fig. 4. This can be used because the optimized SCF calculations suggest that the CC bond length does not change much when the OH bonds are stretched, and that the CC bond can be readily stretched only after proton transfer to form the symmetrical $(HO)_2CCO_2$ geometry. Since the MP2 level transition states have not been determined, and lacking a better alternative, they are assigned the nominal energy values corresponding to optimized 6-31G geometries. These are used in Fig. 4 and as a basis for discussion. The calculated energies and the symmetry of the problem suggests that optimization at MP2 levels will lower the energies for both the III (one-step) and V_b (two-step) proton exchange transition states. While unlikely for MP2 calculations, the sensitivity of III to correlation energy could possibly lower its energy below those calculated for all C_{2v} geometrical configurations when calculations are performed at a higher level. This hypothetical case is dotted into Fig. 4 to emphasize the loss of the two-step proton exchange channel that would occur in this event.

The SCF level calculations can give an idea of the possible atom excursions during proton transfer and decarboxylation reactions. Therefore, atom excursions for the single proton transfer are drawn to scale in Fig. 5, where filled circles give the calculated geometry of oxalic acid monomer (I), open circles give that of $(HO)_2CCO_2$ (V_b), and the geometry of the transition state V_a is indicated by kinks in the lines connecting the atomic positions of I and V_b. It is seen that heavy atom excursions, insofar as they follow minimum energy valleys along the potential energy surface during the proton transfer calculated at the SCF level, are short. There is a tilt of the receiving carboxyl group towards the approaching proton, followed by relaxation upon acceptance of the proton to take positions near their original values. It is worth noting at this time that a carbon kinetic isotope effect can be anticipated for the proton transfer $I \rightarrow V_b$.

Those molecular orbital calculations suggest that proton exchange via single proton transfers is a possible unimolecular reaction channel for oxalic acid monomer. We know

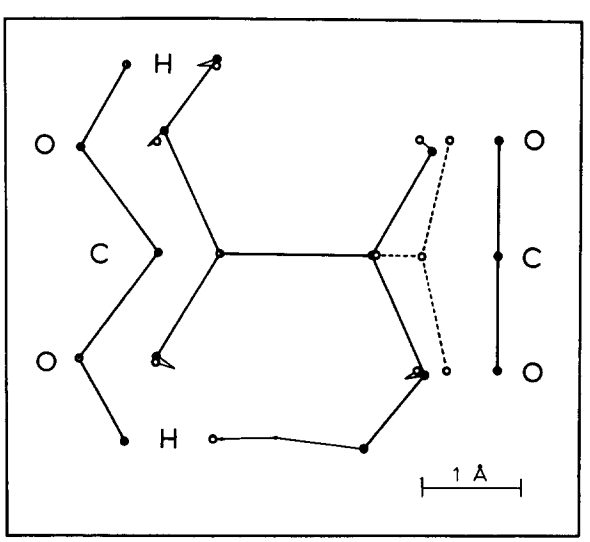

FIG. 5. SCF level geometries for oxalic acid conformer I (filled circles); $(HO)_2CCO_2$ conformer V_b (open circles near I); and transition state V_a (kinks in lines for $I \rightarrow V_b$. Also present (dashed in) is the "CO_2" end of transition state V_c showing the extension of the C–C bond. Finally, geometries of the isolated products dihydroxycarbene and CO_2 are shown (dotted circles).

of no experimental evidence that bears directly on proton exchange measurements for the oxalic acid monomer, however, the present calculations suggest a process that parallels the interpretations of ^{13}C-NMR experiments reported for 2,5-dihydroxy-*p*-benzoquinone by Graf.[24] He performed CNDO calculations to support his analyis of the temperature and solvent dependence of the ^{13}C NMR line shape data in terms of proton exchange via successive, rather than concerted, proton transfers. The experimental lower bound to the activation energy is reported to be about 5 kcal/mol. The barrier calculated for successive proton transfers using CNDO is very much higher than this, but it falls much lower than the corresponding barrier calculated for the symmetric, biprotonic transfer.

E. Unimolecular decarboxylation channels

Lapidus, Barton, and Yankwich[10–13] studied thermal decomposition of oxalic acid vapor in the temperature range 127 to 157 °C, with extension to 180 °C for measurements on carbon-13 isotopomers. The pressures were low, less than 1 Torr, but first order kinetics (to within ± 0.1) was always observed. The reaction has the relatively low activation energy of 31.5 ± 0.8 kcal/mol and follows exactly the stoichiometry $(COOH)_2 \rightarrow HCOOH + CO_2$.[10,11] The mechanism is of considerable interest because the observed kinetic isotope effects indicate mechanistic complexity.[10,13] According to our calculations, decarboxylation appears to occur through C–C bond breaking in a transition state located near geometry V_c. At the SCF level the transition state V_c (Tables I–IV), is calculated to be only 36.5 kcal/mol above conformer I. The "CO_2" end of transition state V_c is dashed in Fig. 5; the dihydroxycarbene end is not shown but the H and O positions fall just to the left of the atom positions marked for I and V_b in Fig. 5.

In Fig. 4 there are pathways for (A) biprotonic exchange with a potential energy barrier listed at 31.9 kcal/mol, (B) proton exchange via successive single proton transfers with a barrier listed at 25.7 kcal/mol, and (C) decarboxylation with a potential barrier listed at 36.6 kcal/mol.

$$\begin{array}{lcccll} \mathrm{I} & \leftrightarrows & \mathrm{III}^{\dagger} & \leftrightarrows & \mathrm{I}' & (\mathrm{A}) \\ \mathrm{I} & \leftrightarrows & \mathrm{V_b}^{\dagger} & \leftrightarrows & \mathrm{I}' & (\mathrm{B}) \\ & & \uparrow\downarrow & & & \\ & & \mathrm{V_c}^{\dagger} & \rightarrow & \mathrm{DHC} + \mathrm{CO_2} & (\mathrm{C}) \\ \mathrm{I} & \leftrightarrows & \mathrm{V_b'}^{\dagger} & \leftrightarrows & \mathrm{I}' & (\mathrm{B}') \\ & & \uparrow\downarrow & & & \\ & & \mathrm{V_c'}^{\dagger} & \rightarrow & \mathrm{DHC} + \mathrm{CO_2} & (\mathrm{C}') \end{array}$$

For thermal dissociation to occur according to those reaction pathways, intramolecular energy associated with proton transfers across the molecule must be converted into C–C bond energy. Similar intramolecular interactions, particularly important when the excitation energy is below the dissociation threshold, can be expected to couple coordinates of the two protons as in reactions (B). Decarboxylation of the thermally excited oxalic acid monomer along the indicated reaction pathways is clearly predicted to be first order, as experimentally observed. To agree with experimental results, however, the dihydroxycarbene (DHC) that is produced must exclusively isomerize to formic acid (FA) and not dissociate to form $H_2 + CO_2$ or $H_2O + CO$.

The temperature dependence of the observed H/D and ^{12}C/^{13}C kinetic isotope effects suggest mechanistic complexity because they possess very strong temperature dependences for their size, and show crossovers from normal to inverse KIE behavior in the relatively small temperature ranges that were investigated.[13] This nonstraightforward type of KIE behavior can be anticipated for a mechanism such as that posed here.[25] The reactions most likely involve tunneling, and the V_c-like decarboxylation transition state and the product molecules are quite dissimilar from reactant molecule I. These factors, particularly those suggesting complex vibrational coupling, are of a type known to contribute to complex temperature dependence for KIEs.[25,26] In view of the availability of experimental observations[10–13] and of the strenuous past efforts that have been made to explain them,[26,27] a calculation of the temperature dependent theoretical KIEs using 6-31G level force fields appears to be a worthwhile future endeavor for the oxalic acid system. The arguments presented here appear valid even if the energy of III should be found low enough to eliminate the V_b-like PES saddle point.

While much work remains to be performed both experimentally and computationally on oxalic acid monomer, it is noted that recent experimental results on the decarboxylation reactions of pyruvic,[28] and acrylic and methacrylic,[29] acid monomers by Rosenfeld and Weiner are intimately tied to the computational results presented here for oxalic acid monomer. Analysis of infrared fluorescence from the CO_2 produced by eximer laser photolysis of pyruvic acid led these authors to postulate the presence of methylhydroxycarbene as a reaction intermediate that is subsequently isomerized to the acetaldehyde stoichiometric product. The experimentally based notion that methylhydroxycarbene is produced from pyruvic acid monomer requires a proton transfer and dissociation channel that are completely analogous to the situation involving a single proton transfer that we have discovered to occur in these computations on the oxalic acid monomer.

Because of the importance of the behavior of dihydroxycarbene to the proposed reaction mechanism, this substance was also briefly studied as part of the present research.

F. Dihydroxycarbene

The properties of dihydroxycarbene have already been studied by *ab inito* quantum mechanical methods. Feller, Borden, and Davidson[30,31] used various basis levels up to a double zeta set comparable to 6-31G**(5*d*), and also calculated configuration interaction contributions as part of their investigation. The computations yield an activation barrier of 52.6 kcal/mol for the 1,2 H atom shift in dihydroxycarbene to form formic acid monomer at the DZP level, and the much higher value of 76.8 kcal/mol for dissociation to form $H_2 + CO_2$ at the same level. Barriers for internal rotation of the OH groups were also calculated to be high. With the STO-3G basis the barrier is 42.8 kcal/mol and the planar "S", "W", and "U" configurations of $(HO)_2C$: are at 0.0, 0.9, and 7.8 kcal/mol, respectively. The cited calculations

probably overestimate the barrier heights, but clearly a basic stability for the isolated dihydroxycarbene molecule is suggested. The dissociation channel to form $H_2O + CO$ was not investigated by Feller *et al.* but, presumably, its activation energy is also high.

The energy of the planar conformer

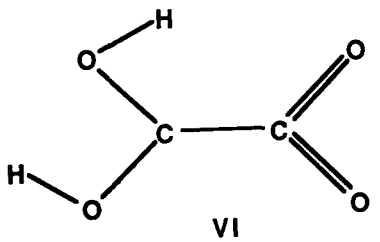

VI

the *S* form of $(HO)_2CCO_2$, was calculated at the 6-31G level and found to be 8.6 kcal/mol above the energy of conformer V_b (the *W* form), as listed in Tables I, III, and IV. The energetics for decarboxylation of this $(HO)_2CCO_2$ conformation were not investigated.

The barriers calculated for unimolecular reactions of dihydroxycarbene are higher than the activation energy needed for the dissociation of oxalic acid monomer. They suggest (a) the desirability of an experimental search for the presence of dihydroxycarbene as a product of the dissociation of oxalic acid monomer under near-collisionless conditions, e.g., laser photolysis in a supersonic molecular beam, and (b) the need for further computational research to investigate the possibility for a low energy channel for its isomerization under conditions of thermal reaction. No studies capable of detecting dihydroxycarbene as a transient in dissociating oxalic acid vapor have been performed to date to our knowledge.

For comparison with the results of Feller *et al.* on dihydroxycarbene,[28,29] and comparison with the above calculations on oxalic acid monomer, the activation barrier for the unimolecular 1,2 H atom shift of dihydroxycarbene was calculated at the 6-31G, 6-31G**(5*d*), and MP2/6-31G*(5*d*) levels. The relevant geometries and energies obtained are listed in Tables I–IV. The results agree with the conclusions of Feller *et al.* that, overall, a basic stability can be expected for the isolated dihydroxycarbene molecule. The barrier for the analogous 1,2 H shifting reaction of hydroxycarbene, HOCH, to form formaldehyde is of the same order of magnitude according to the extensive calculations reported by Goddard and Schaeffer.[32]

The proton excursion for the 1,2 H atom shift to form *trans* formic acid is drawn to scale for SCF geometry in Fig. 6. The energy barrier is higher, and the proton excursion much longer (well over 3 Å), than is the case for the single proton transfer in oxalic acid monomer drawn in Fig. 4.

Thermal dissociation of oxalic acid monomer at temperatures up to about 180 °C result in the quantitative formation of formic acid and CO_2.[10,13] Under more energy-rich conditions, e.g., UV photolysis or CO_2 laser multiphoton absorption, an alternative channel to form $H_2O + CO$ is opened. The $H_2O + CO$ is reported to come from the oxalic acid and not from subsequent dissociation of formic acid generated from the oxalic acid.[14] Unfortunately, a dissociation channel to form $H_2O + CO$ from dihydroxycarbene has not yet been investigated theoretically. Production of $H_2 + CO_2$ was studied theoretically, but there does not appear to be a significant experimental channel to form H_2 in the oxalic acid thermal decomposition.

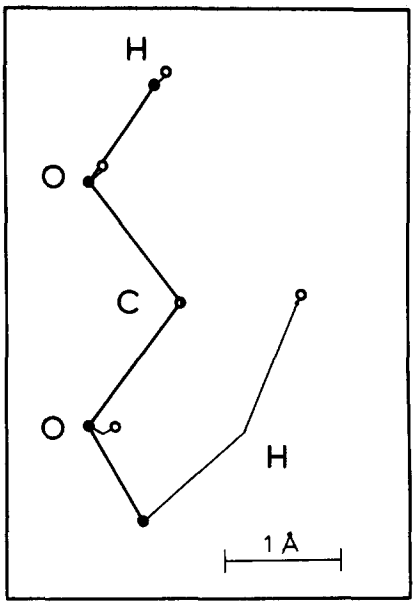

FIG. 6. SCF level geometries for dihydroxycarbene (filled circles) *cis* formic acid (open circles), and the transition state between them (kinks).

The high energy barriers, calculated for both the unimolecular isomerization and the dissociation of dihydroxycarbene to form $H_2 + CO_2$ suggest the possible existence of an alternative biomolecular process for isomerization of dihydroxycarbene under thermal reaction conditions. A subsequent bimolecular reaction of dihydroxycarbene produced according to the above dissociation channels does not affect the first order reaction kinetics for decarboxylation of oxalic acid. One of several plausible possibilities for bimolecular isomerization of dihydroxycarbene is via proton exchanges occurring in a collisional complex, e.g.,

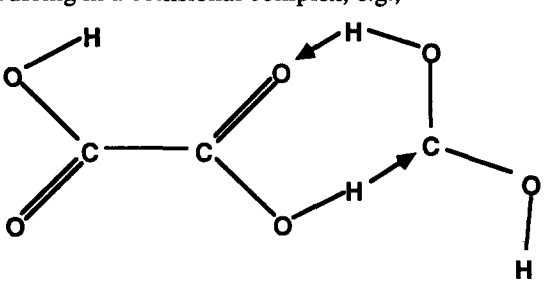

The various oxalic acid conformers are present in sufficient abundance in the hot vapor of the thermal decarboxylation reaction. The energetics for this proton exchange reaction have not yet been investigated using MO theory, but a low activation barrier seems likely to occur. In a somewhat similar situation MO calculations of a double proton transfer in a transient $H_2O \cdot HCOOH$ intermediate were found to drastically lower the activation barrier for decarboxylation of formic acid monomer. The lowest barrier calculated for unimolecular decarboxylation was 77.6 kcal/mol, as compared to only 18.7 kcal/mol for the collisional, H_2O catalyzed, process.[33]

Tables III and IV, and Fig. 3 show the calculated energy

of the four-center transition state for 1,2 H shifting in dihydroxycarbene. They also give the energy values for the resulting *trans* formic acid (both with the energy of CO_2 added on). The reaction is exothermic experimentally, with $H = -35$ kcal/mol. The energy of the lowest energy products, *trans* formic acid and CO_2, is -6.5 kcal/mol relative to conformer I at the 6-31G level and -13.3 kcal/mol at the 6-31G**(5*d*) level.

IV. FURTHER DISCUSSION AND CONCLUSIONS

These molecular orbital calculations provide guidelines for interpreting the behavior of the oxalic acid monomer as it has been observed in experiments performed to date, and they suggest possible avenues for future experimental research, e.g., using the oxalic acid monomer to produce dihydroxycarbene under molecular beam sampling conditions. Vibrational frequencies for conformations other than I and II were not calculated in this research and, hence, zero point vibrational contributions to the various barrier heights are not made and kinetic isotope effects for the decarboxylation reaction are not calculated.

In concluding this article, the basic results of this MO study are summarized.

(A) Rotational isomerization is predicted to be important for the oxalic acid monomer and, at the SCF level, a shallow *gauche* minimum in the potential energy function is calculated to occur for the symmetrical, non-hydrogen-bonded, isomer. The rotational conformation with lowest energy is the intramolecularly hydrogen bonded structure I, but potential energy values for all planar conformations reached by internal rotations are estimated to occur within a range of about 2 kcal/mol of one another.

(B) Taking correlation energy into account at the MP 2 level, the symmetric, concerted, intramolecular transfer of protons between the equivalent wells of the double minimum global potential energy function of oxalic acid monomer is predicted to have a higher activation energy than a competing proton exchange mechanism involving successive transfer and a lower activation energy than the unimolecular decarboxylation reaction. The latter two transition states have not been determined at the MP2 level, but they will be of the form $(HO)_2CCO_2$, with C_{2v} symmetry.

Single point calculations using critical point geometries for III, V_b, and V_c optimized at the 6-31G level (i.e., MP2/6-31G*(5*d*)||HF/6-31G) yield energy values of 31.9, 25.7, and 36.6 kcal/mol. These values are taken as the best presently available estimates for the corresponding transition state energies.

(C) The observed kinetics of the thermal decarboxylation of oxalic acid monomer in the vapor phase can be rationalized through dissociation of a $(HO)_2CCO_2$-type transition state wtih C_{2v} symmetry (called V_c) reached by a proton transfer. The dihydroxycarbene dissociation product must subsequently isomerize to formic acid monomer, possibly through a bimolecular process involving proton exchanges with oxalic acid or other monomer. There is no formation of $H_2 + CO_2$ or of $H_2O + CO$ under conditions of the thermal decomposition of oxalic acid.[11–13] Under experimental conditions that provide a higher input of energy to the sample molecule than reached by thermal energies up to 180 °C, the products H_2O and CO are experimentally observed along with HCOOH and CO_2, but there is no more than a trace of H_2.[14] The H_2O and CO can result from dissociation of dihydroxycarbene or, possibly, from dissociation of $(HO)_2CCO_2$ configurations through some as yet uninvestigated higher energy, perhaps nonplanar, channel.

ACKNOWLEDGMENTS

The computer center of the Philadelphia College of Textiles and Science provided generous grants of computer time for this research which was also supported, in part, by the Robert A. Welch Foundation.

[1]S. Shibata and M. Kimura, Bull. Chem. Soc. Jpn. **27**, 485 (1954).
[2]Z. Nahlovska, B. Nahlovsky, and T. G. Strand, Acta Chem. Scand. **24**, 2617 (1970).
[3]H. Murata and K. Kawai, J. Chem. Phys. **25**, 589 (1956).
[4]B. M. Pava and F. B. Stafford, J. Phys. Chem. **72**, 4628 (1968).
[5]L. Bardet, G. Fleury, and V. Tabacik, C. R. Acad. Sci. Ser. B **270**, 1277 (1970).
[6]B. C. Stace and C. Oralratmanee, J. Mol. Struct. **18**, 339 (1973).
[7]R. L. Redington and T. E. Redington, J. Mol. Struct. **48**, 165 (1978).
[8]R. L. Redington, J. Liang, and C. W. Bock (to be published).
[9]R. A. Back, Can. J. Chem. **62**, 1414 (1984).
[10]G. Lapidus, D. Barton, and P. E. Yankwich, J. Phys. Chem. **68**, 1863 (1964).
[11]G. Lapidus, D. Barton, and P. E. Yankwich, J. Phys. Chem. **70**, 407 (1966).
[12]G. Lapidus, D. Barton, and P. E. Yankwich, J. Phys. Chem. **70**, 1575 (1966).
[13]G. Lapidus, D. Barton, and P. E. Yankwich, J. Phys. Chem. **70**, 3135 (1966).
[14]S. Yamamoto and R. A. Back, J. Phys. Chem. **89**, 622 (1985).
[15]C. VanAlsency, V. J. Klimkowski, and L. Schafer, J. Mol. Struct. (Theochem) **109**, 321 (1984).
[16]J. S. Binkley, M. J. Frisch, D. J. DeFrees, K. Raghavachari, R. A. Whiteside, H. B. Schlegel, and J. A. Pople, Carnegie–Mellon Univ., Pittsburgh, Pa. 15213 (1983).
[17]K. Saito, T. Kakumoto, H. Kuroda, S. Torii, and A. Imanura, J. Chem. Phys. **80**, 4989 (1984).
[18]K. Ohno and K. Morokuma, J. Mol. Struct. **134** (Theochem, 27), 1 (1985). This volume contains 1548 literature references to *ab initio* calculations published mostly in 1984.
[19]C. Moller and M. S. Plesset, Phys. Rev. **46**, 678 (1934).
[20]W. H. Hocking, Z. Naturforsch. Teil A **31**, 1113 (1976).
[21]I. A. Godunov, A. V. Abramenkov, and A. I. Tyulin, J. Struct. Chem. **24**, 194 (1983).
[22]C. W. Bock and Y. Panchenko (to be published).
[23]The situation is summarized by Y. Osamura and H. F. Schaeffer III, J. Chem. Phys. **74**, 4576 (1981).
[24]F. Graf, Chem. Phys. Lett. **62**, 291 (1979).
[25]W. A. Van Hook, in *Isotope Effects in Chemical Reactions*, edited by C. J. Collins and N. S. Bowman (Van Nostrand Reinhold, New York, 1971), Chap. 1.
[26]T. T.-S. Huang, W. J. Kass, W. B. Buddenbaum, and P. E. Yankwich, J. Phys. Chem. **72**, 4431 (1968).
[27]W. B. Buddenbaum, H. A. Haleem, and P. E. Yankwich, J. Phys. Chem. **71**, 2929 (1967).
[28]R. N. Rosenfeld and B. R. Weiner, J. Am. Chem. Soc. **105**, 3485 (1983).
[29]R. N. Rosenfeld and B. R. Weiner, J. Am. Chem. Soc. **105**, 6233 (1983).
[30]D. Feller, W. T. Borden, and E. R. Davidson, J. Chem. Phys. **71**, 4987 (1979).
[31]D. Feller, W. T. Borden, and E. R. Davidson, J. Comput. Chem. **1**, 158 (1980).
[32]J. D. Goddard and H. F. Schaeffer III, J. Chem. Phys. **70**, 5117 (1979).
[33]P. Ruelle, U. W. Kesselring and H. Nam-Tran, J. Am. Chem. Soc. **108**, 371 (1986).